Guanidinium Chloride Molecular Diffusion in Aqueous and Mixed Water−Ethanol Solutions

ARTICLE *in* THE JOURNAL OF PHYSICAL CHEMISTRY B · AUGUST 2008

Impact Factor: 3.3 · DOI: 10.1021/jp8030336 · Source: PubMed

Guanidinium Chloride Molecular Diffusion in Aqueous and Mixed Water−Ethanol Solutions

G. Gannon, J. A. Larsson, J. C. Greer, and D. Thompson*

Tyndall National Institute, Lee Maltings, Prospect Row, Cork, Ireland

Received: April 8, 2008; Revised Manuscript Received: May 9, 2008

Solutions containing guanidinium chloride (GdmCl), or equivalently guanidine hydrochloride (GdnHCl), are commonly used to denature macromolecules such as proteins and DNA in, for example, microfluidics studies of protein unfolding. To design and study such applications, it is necessary to know the diffusion coefficients for GdmCl in the solution. To this end, we use molecular dynamics simulations to calculate the diffusion coefficients of GdmCl in water and in water−ethanol solutions, for which no direct experimental measurements exist. The fully atomistic simulations show that the guandinium cation Gdm^+ diffusion decreases as the concentration of both Gdm^+ and ethanol in the solution increases. The simulations are validated against available literature data, both transformed measured viscosity values and computed diffusion coefficients, and we show that a prudent choice of water model, namely TIP4P-Ew, gives calculated diffusion coefficients in good agreement with the transformed measured viscosity values. The calculated Gdm^+ diffusion behavior is explained as a dynamic mixture of free cation, stacked cation, and ion-paired species in solution, with weighted contributions to Gdm^+ diffusion from the stacked and paired states helping explain measured viscosity data in terms of atom-scale dynamics.

1. Introduction

Microfluidics is becoming widely used in areas as diverse as medical diagnostics, chromatography, and drug discovery.[1–5] One very promising application is the unfolding (denaturation) of proteins in microfluidic cells,[2,6,7] the regulation of which requires a strict control on the diffusion coefficient of the denaturing agent. Denaturants act by disrupting the three-dimensional structure of macromolecules leading for example to protein unfolding from the native state. Understanding how proteins fold, misfold, and unfold is a major goal of molecular biology and is crucial for the design of drug molecules tailor-made for the treatment of neurodegenerative disorders such as Alzheimer's, Parkinson's, and prion disease.[8–11]

Three classic chaotropic agents commonly used to denature proteins are urea, sodium perchlorate, and guanidinium chloride (GdmCl), and although the diffusion coefficients of urea and sodium perchlorate are both well-known,[12,13] the diffusion of the GdmCl salt has yet to be measured experimentally. GdmCl diffusion coefficients have been computed from molecular simulations with GdmCl solvated in a variety of water models, namely, SPC/E, SPC, and TIP3P water,[14] but no values exist however for the arguably superior[15] TIP4P and TIP4P-Ew water models or for models incorporating ethanol—both aqueous and water−ethanol solutions of GdmCl have been used to induce protein unfolding.[16,17] GdmCl is also used in nucleic acid purification[18] and microfluidic nucleic acid probe assays,[19] and substituted guanidines are used as fuel stabilizers;[20] all of these applications will benefit from a deeper knowledge of GdmCl diffusion.

It is well-known that the degree to which a protein unfolds is dependent on the concentration of the denaturant,[21] and for example, to gauge the equilibration time in a T-channel of a microfluidic system, one must know the diffusion coefficient of the solutions involved. In the present work, we report the concentration-dependent diffusion coefficient of GdmCl in a range of water and water−ethanol solutions, a crucial step toward optimizing the use of GdmCl as a denaturant in microfluidics and for providing a benchmark for the design of denaturants with tailored diffusion properties. Similar molecular simulations have been used to complement experimental studies of protein denaturation, see, for example, refs 22 and 23. We used fully atomistic molecular dynamics (MD) computer simulations to compute GdmCl diffusion over a range of typical microfluidics concentrations and solvents.[16,17] Control simulations were also performed for neat water and neat ethanol, and generated diffusion coefficients were compared with the literature values.

2. Methods

A series of guanidinium (protonated guanidine) Gdm^+ cations with chloride Cl^- counterions were solvated by using three different water models (see below) and an ethanol model, to simulate a typical range of GdmCl solutions for microfluidics.[16,17] The molecular formula of Gdm^+ is $C(NH_2)_3^+$. Standard CHARMM22 force field parameters[24] were used for GdmCl and ethanol and, where available, for the different water models. The GdmCl solutions together with neat water and neat ethanol systems were simulated within the constant number of particles, constant pressure, and constant temperature (*NPT*) ensemble. Periodic boundary conditions are applied; that is, the simulation cell is replicated periodically in all directions. Temperature was controlled by using the Hoover algorithm, and Ewald summation was used to calculate the electrostatic interactions. The leapfrog integrator was used to integrate the equations of motion.

Following approximately 0.5 ns of equilibration and thermalization (see equilibration data and density profiles in the Supporting Information), 1.6 ns of free MD was performed for

* Author to whom all correspondence and requests for reprints should be addressed. Phone: +353-21-490-4327. Fax: +353-21-427-0271. E-mail damien.thompson@tyndall.ie.

10.1021/jp8030336 CCC: $40.75
Published on Web 07/09/2008

TABLE 1: Measured[30] and Computed Self-Diffusion Coefficients for Water by Using Three Alternative Water Models[28,29]

	diffusion coefficient[a] (10^6 cm^2/s)
experiment[30]	23.0 ± 0.5
TIP3P	52.7 ± 0.6
TIP4P	35.4 ± 0.8
TIP4P-Ew	19.9 ± 0.4

[a] Values are averaged over the last 1.6 ns of 2.1 ns trajectories, sampling every 10 ps for a total of 160 datapoints with time-averaged standard deviations as shown.

each system. The solvated GdmCl systems consisted of 16, 32, 48, 64, 80, and 96 salt molecules solvated in the different water models. A total of 16-molecule and 32-molecule salt solutions were also simulated with 28, 56, 84, and 112 ethanol molecules, which were then solvated with water to give in all cases a cubic box with an initial edge length of 30 Å. We thus built starting configurations corresponding to 1, 2, 3, 4, 5, and 6 M GdmCl concentrations in water and 1 and 2 M GdmCl concentrations in 10, 20, 30, and 40% ethanol solutions. Bonds involving hydrogen were constrained to their experimental lengths with the SHAKE algorithm[25] and a 1 fs time step was used for dynamics. We used the CHARMM program[26] version c31b2 for all calculations.

Because of the variety of water models available and the proven impact of water model choice on diffusion coefficients,[27] a range of water models were tested. The models used were TIP3P,[28] TIP4P,[28] and TIP4P-Ew[29] as parametrized for the CHARMM22 force field[24] and by using new parameters where necessary for TIP4P-Ew.[27,29] TIP3P is a three-site model with the charges placed on the atoms,[28] whereas the TIP4P models have four sites with an extra charge placed along the bisector of the hydrogen atoms.[28] TIP4P-Ew is an implementation of the TIP4P model optimized for use with the Ewald method of treating charge in a periodic system.[29]

To calculate diffusion coefficients, we used the Einstein Diffusion equation

$$D = \frac{1}{2dt} \lim_{t \to \infty} \frac{\langle [\underline{r}(t_0 + t) - \underline{r}(t_0)]^2 \rangle}{t} \quad (1)$$

where D is the diffusion coefficient and d is the dimensionality of the system. The numerator is the mean square displacement, and the angled brackets indicate an ensemble average is to be taken. Care must be taken to ensure that only fully equilibrated data, with many instantaneous positions (MD snapshots) over a long time period, are used in calculating D; the data given in the Supporting Information show that we only use equilibrated data and that we sample for sufficiently long times (in this case, 1.6 ns) to ensure that our computed diffusion coefficients are well converged with respect to time.

3. Results and Discussion

3.1. Water Self-Diffusion Coefficients. Before calculating GdmCl diffusion, we first tested the ability of three alternative water models to reproduce the experimental water self-diffusion coefficient, with results given in Table 1. The computed self-diffusion coefficient D for the TIP3P model is 52.7×10^{-6} cm^2/s, more than twice the experimental value for water of 23.0×10^{-6} cm^2/s[30] but typical of computed TIP3P values.[27] Similarly, the computed TIP4P water D of 35.4×10^{-6} cm^2/s is also high when compared with experiment but is again similar to computed values previously obtained by using this model.[27] TIP4P-Ew was parametrized specifically to model water diffusion,[29] and we see in Table 1 that TIP4P-Ew water has a computed D of 19.9×10^{-6} cm^2/s, approximately 90% of the measured value and significantly better than the TIP3P and TIP4P models which give 230 and 150% of the experimental value, respectively.

3.2. GdmCl Diffusion in Water. Table 2 gives the GdmCl diffusion coefficient D in aqueous solution, specifically the Gdm^+ cation D, over a range of salt concentrations typically used in denaturing experiments,[16] and Figure 1 plots the relationship between diffusion coefficient and GdmCl concentration for the three different water models. Note that the volume of the *NPT* simulation boxes (see Methods) changed to give a homogeneous density profile for each solution (as shown in the Supporting Information, the average volume becomes equilibrated within 0.6 ns), accounting for the slight differences in individual concentration values sampled for the different water models as shown in the horizontal axis of Figure 1. We observed average increases of ~5% for the TIP4P and TIP4P-Ew water models over the simulations, with a more pronounced increase of approximately 15% for TIP3P. Individual concentrations used in to generate the data in Figure 1 are calculated in each case from the number of GdmCl molecules, and the cell volumes are averaged over 1.6 ns of free dynamics.

Extracting a linear relationship from the GdmCl in TIP4P-Ew water datapoints in Figure 1 yields the relation $D = (-0.91 \times 10^{-6})[C] + (7.4 \times 10^{-6})$ cm^2/s, where D is the diffusion coefficient, $[C]$ is the molar concentration, and the linear regression coefficient R^2 is found to be 0.97. Extrapolating to low, sub-1 M concentrations, the diffusion coefficient approaches 7.4×10^{-6} cm^2/s, which may approximate the diffusion coefficient at infinite dilution. TIP3P and TIP4P, the alternative water models shown to be less-suited for water self-diffusion studies (Table 1 and ref 27), both give significantly sharper reductions in diffusion with increased GdmCl concentration, illustrating the importance of choosing the right solvent model when calculating solute diffusion coefficients. Table 3 shows that the results obtained here are similar to previously computed values in the literature[14] for a 6 M GdmCl solution; the results for TIP3P overlap, and those for the TIP4P-Ew and SPC/E[14] models are very close.

Figure 2 compares our computed GdmCl in TIP4P-Ew water diffusion coefficients with transformed experimental viscosity values.[31] Two methods were employed to generate diffusion coefficients from the experimental viscosity data. In Method One, the experimental values are transformed to diffusion coefficients by using the spherical version[32] of the Stokes−Einstein diffusion equation

$$D = \frac{k_B T}{6\pi\eta a} \quad (2)$$

where D is the diffusion coefficient, k_B is Boltzmann's constant, T is the temperature, η is the viscosity, and a is an effective molecular radius, set here to 3.3 Å for Gdm^+, comprising the sum of the carbon−nitrogen bond length (1.4 Å) and the nitrogen van der Waals radius (1.9 Å). In Method Two, the spherical Stokes−Einstein diffusion equation (eq 2) was combined, as explained below, with the randomly moving ellipsoid version[32]

$$D = \frac{k_B T}{6\pi\eta a / \ln(2a/b)} \quad (3)$$

where a is half the length of the ellipsoid and b is half the width of the ellipsoid. Three spheres and one ellipsoid were used to

TABLE 2: Calculated GdmCl Diffusion Coefficients (10^6 cm^2/s) as a Function of Starting Concentration by Using Three Different Water Models[a]

	[GdmCl], M					
	1	2	3	4	5	6
TIP3P	13 ± 3	11 ± 1	7.9 ± 1	5.1 ± 1	3.6 ± 0.2	2.1 ± 0.2
TIP4P	9.3 ± 2	9.4 ± 1	6.7 ± 0.7	5.4 ± 0.3	4.0 ± 0.3	3.2 ± 0.2
TIP4P-Ew	6.2 ± 2	5.4 ± 0.6	5.0 ± 0.6	3.3 ± 0.6	2.4 ± 0.2	2.0 ± 0.1

[a] As explained in the text, equilibrated solution concentrations increased by approximately 15% (TIP3P) or 5% (TIP4P, TIP4P-Ew) relative to the starting concentrations. Values given are averaged over the last 1.6 ns of 2.1 ns trajectories, sampling every 10 ps for a total of 160 datapoints with time-averaged standard deviations as shown.

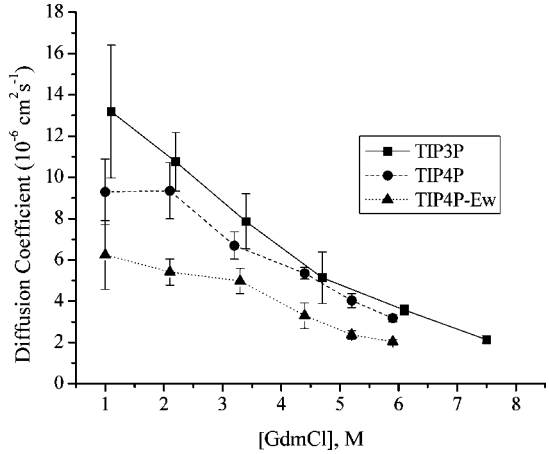

Figure 1. GdmCl diffusion in water as a function of concentration for three different water models. The error bars represent time-averaged standard deviations, and datapoints for each data set are connected to guide the eye.

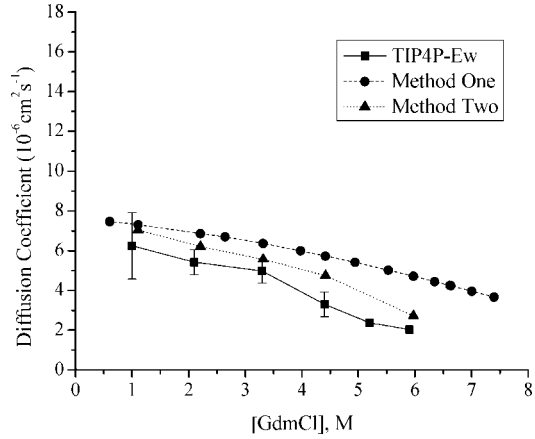

Figure 2. GdmCl diffusion in TIP4P-Ew water as a function of concentration compared with transformed measured viscosity values[31] for free Gdm^+ ions (Method One) and weighted Gdm^+ complexes (Method Two), with the models explained in the text. The error bars represent time-averaged standard deviations, and datapoints for each data set are connected to guide the eye.

TABLE 3: Comparsion of the Computed Diffusion Coefficient of Gdm^+ Ion at Approximately 6M (Actual Time-Averaged Concentration Given in Brackets) Obtained in this Work (see Figure 1) and in Weerasinghe & Smith[14]

this work		Weerasinghe & Smith[14,a]	
water model	diffusion coefficient (10^6 cm^2/s)	water model	diffusion coefficient (10^6 cm^2/s)
TIP3P	3.6 ± 0.2 (6.1 M)	TIP3P	3.4
TIP4P	3.2 ± 0.2 (5.9 M)	SPC	2.5
TIP4-Ew	2.0 ± 0.1 (5.9 M)	SPC/E	1.8

[a] Weerasinghe & Smith[14] simulated 230 Gdm^+ ions in 1209 water molecules for 5 ns, at 1 atm and 300 K.

transform the experimental viscosity data[31] into diffusion coefficients, as illustrated in Figure 3.

The first sphere shown in Figure 3a represents the free Gdm^+ ion with a sphere radius $a = 3.3$ Å (as above). The second sphere shown in Figure 3b is based on the dimensions of a Gdm^+ ion participating in a stacking conformation, an example of which is shown in Figure 4 and discussed in detail in recent simulation work.[33] We modeled this effective Gdm^+:Gdm^+ cation dimerization by using eq 2 and a sphere with radius $a =$ 4.1 Å, comprised of half the Gdm^+:Gdm^+ separation (2.1 Å, from the first peak at 4.1 Å in the $g_{cc}(r)$ radial distribution function shown in Figure 5) plus the carbon van der Waals radius[24] (2.0 Å). The ellipsoid shown in Figure 3c is based on the dimensions of a Gdm^+ cation participating in an ion pair with a Cl^- anion, as illustrated in Figure 4 and described in detail in ref 33, with Cl^- coordinating principally in the plane of Gdm^+. This gives parameters for eqn 3 of $a = 4.9$ Å and $b = 2.0$ Å. As shown in Figure 3c, *2a* is the sum of 3.3 Å, from the free Gdm^+ sphere in Figure 3a, plus 4.1 Å, from the first peak at 4.1 Å in the $g_{CC}(r)$ radial distribution function in Figure 6, plus the Cl^- van der Waals radius of 2.3 Å. The additional ellipsoid parameter in eq 3, $b = 2.0$ Å, corresponds to half the ellipsoid width in Figure 3c and is thus equal to the carbon van der Waals radius. The third sphere shown in Figure 3d represents a Gdm^+ ion participating simultaneously in a stack and an ion pair, an example of which is shown in Figure 4, with $a = 4.9$ Å, from the Gdm^+:Cl^- ellipsoid described above. The spheres and ellipsoid were weighted according to their occupancies throughout the equilibrated simulations, as given in Table 4.

The transformed experimental viscosity values from Method One, corresponding to the free Gdm^+ ion, and Method Two, corresponding to a weighted mixture of free and complexed Gdm^+ as described above, together with our computed GdmCl diffusion curve in TIP4P-Ew water, are compared in Figure 2. The Gdm^+ complex curve, labeled Method Two in Figure 2, depends on the relative weights of the various Gdm^+ complexes over the range of concentrations simulated (Table 4); therefore, it has fewer data points than the Gdm^+ ion curve, labeled Method One in Figure 2, which assumes uncomplexed, free Gdm^+ ions. The relative weights of the different free and complexed Gdm^+ states vary as a function of concentration, as shown in Table 4. For example, as the GdmCl concentration increases, so does the population of Gdm^+:Cl^- ion pairs. In the 1.0 M solution, Cl^- is coordinated to Gdm^+ 30% of the time, whereas in the 5.9 M solution, Cl^- coordinates Gdm^+ 140% of the time (interpreted as a dynamic equilibrium between mono- and multicoordinated states).

We find good agreement between our computed *D* values obtained from the MD simulations and the transformed measured viscosity values[31] obtained from both the free Gdm^+ ion and the Gdm^+ complexed ion models (Method One and Method

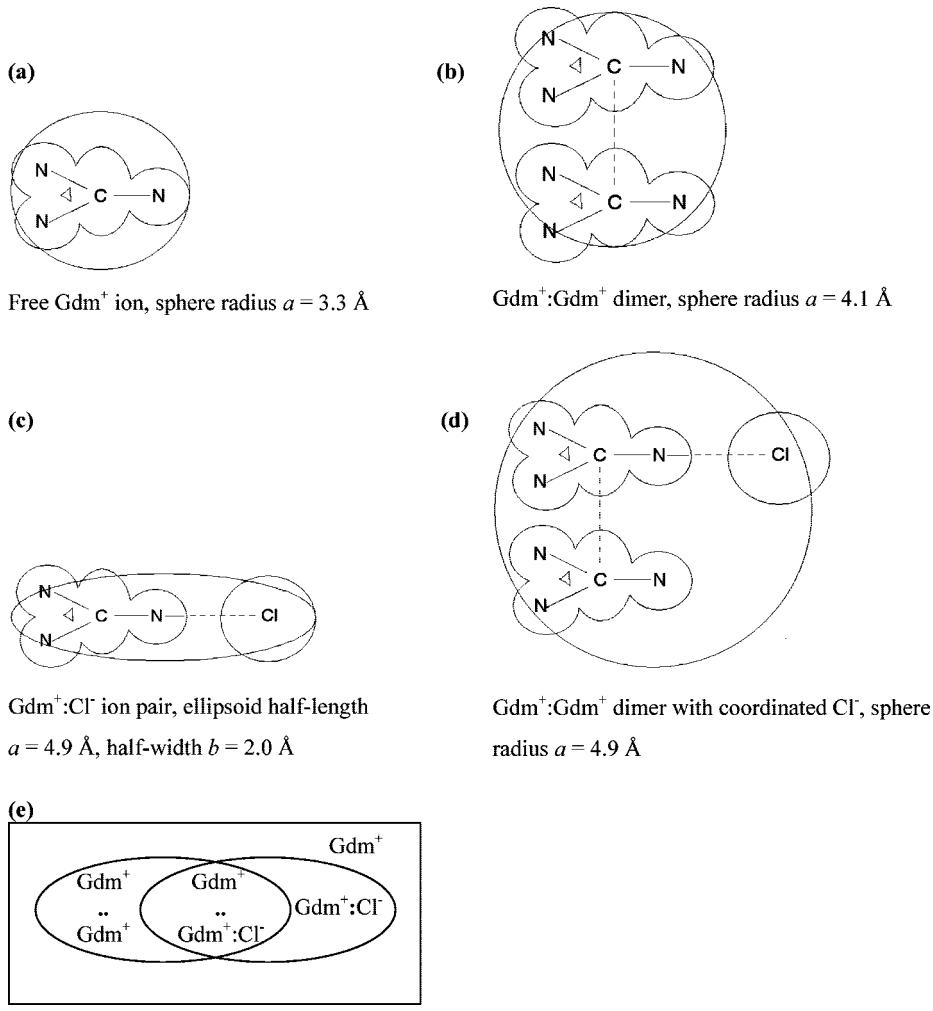

Figure 3. Panels (a), (b), (c), and (d) show schematic representations of the three spheres and one ellipsoid used to describe the various free and complexed Gdm^+ diffusing species in GdmCl solutions, with a and b values as labeled fitted to eqs 2 and 3 to transform measured viscosity values[31] into diffusion coefficients. The Venn diagram in panel (e) illustrates the contributions of the four different species (with actual concentration-dependent weights calculated from the data in Table 4): the free Gdm^+ ion, the Gdm^+:Gdm^+ dimer stack, the Gdm^+:Cl^- ion pair, and the Gdm^+:Gdm^+ dimer with coordinated Cl^-. Reference 33 shows that the Gdm^+:Gdm^+ dimer is the predominant $(Gdm^+)_{n>1}$ multimer in solution. Hydrogens are omitted for clarity.

TABLE 4: Trajectory-Averaged Overall Occupancies of Gdm^+:Gdm^+ dimers, Gdm^+ Cl^- Ion Pairs, Gdm^+:Gdm^+ Dimers with Coordinated Cl^-, and Free Gdm^+ in TIP4P-Ew Water. Gdm^+:Gdm^+ and Gdm^+:Cl^- (Separations of ≤5.1 Å and ≤5.4 Å, respectively, were considered complexes, from Figures 5 and 6 and ref 33)[a]

	[GdmCl], M					
	1.0	2.1	3.3	4.4	5.2	5.9
dimer occupancy (%)	7	15	15	0	0	0
ion-pair occupancy (%)	27	35	35	30	24	0
dimer with Cl^- occupancy (%)	3	15	35	70	96	140
free Gdm^+ occupancy (%)	63	35	15	0	0	0

[a] Values given are averaged over the last 1.6 ns of 2.1 ns trajectories, sampling every 10 ps for a total of 160 datapoints.

Two, respectively, in Figure 2). As the concentration of GdmCl increases, the diffusion coefficient decreases, as is anticipated. The quantitative agreement between the computed diffusion coefficient and the transformed measured viscosity values deteriorates at higher GdmCl concentrations, and the Gdm^+ complexed ion model captures this behavior better than the single Gdm^+ ion model, indicative of the increased contributions from stacking and ion pairing at higher concentrations. Both methods use approximations in transforming the data. In Method One, the Gdm^+ ion is modeled as a sphere, and in Method Two, the Gdm^+ complexed ion is modeled as a weighted combination of spheres and an ellipsoid. Both models serve as approximations to the true dynamic structure of the diffusing species. It is therefore considered that the (as yet unmeasured) experimental diffusion coefficient is better matched by the simulation, corresponding to the data labeled TIP4P-Ew in Figure 2, than by either transformed data set because of the structural complexities within the physical solutions.

3.3. Ethanol Self-Diffusion and GdmCl Diffusion in Water–Ethanol Solutions. Table 5 shows the computed ethanol self-diffusion coefficient, in excellent agreement with experimental measurements[34] and illustrating the relative ease with which diffusion may be modeled for the less polar, organic solvent. Table 6 shows how the diffusion of GdmCl varies over a range of typical microfluidics salt and ethanol concentrations.[17] Our computed D values show that the diffusion coefficient of GdmCl decreases with increasing GdmCl concentration (Figure 7) and also, comparing the 1.1 and 2.2 M solutions, that the higher the concentration of ethanol, the slower Gdm^+ appears to

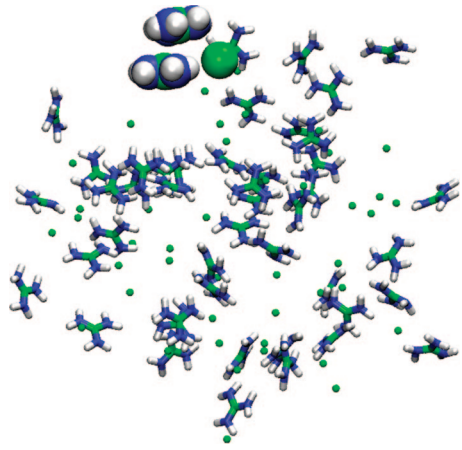

Figure 4. Two Gdm^+ ions and a Cl^- ion are highlighted, participating in a Gdm^+:Gdm^+ dimer with coordinated Cl^-. This is the most complex species considered in the present study; non-Cl^--coordinated Gdm^+:Gdm^+ dimers and single Gdm^+:Cl^- ion pairs were also observed in the simulations, as described in the text. Snapshot taken at the end of a 2.1 ns simulation of 2.1 M GdmCl in TIP4P-Ew water. Carbon and chlorine atoms are colored green, nitrogens are colored blue, and hydrogens are colored white.

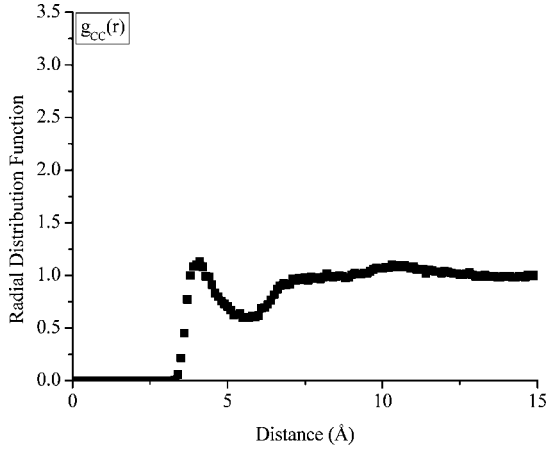

Figure 5. Radial distribution function of the carbon atoms describing the distribution of Gdm^+ cations in solution, $g_{cc}(r)$, from a 2.1 ns simulation of 3.3 M GdmCl in TIP4P-Ew water.

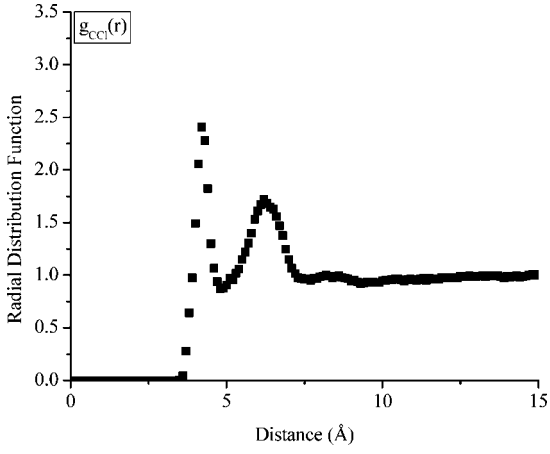

Figure 6. Radial distribution function of Cl^- anions around the carbon of Gdm^+ cations, $g_{CC}(r)$, from a 2.1 ns simulation of 3.3 M GdmCl in TIP4P-Ew water.

diffuse, although there is some overlap in the data. The equilibration time for a T-channel in a microfluidics cell is inversely proportional to the diffusion coefficient,[35] and as an illustrative example, as one increases the concentration of ethanol from 1.1 to 4.2 M (for the 1.1 M GdmCl solute concentration), the diffusion coefficient drops from 6.2×10^{-6} to 3.1×10^{-6} cm^2/s, as shown in Figure 7, doubling the T-channel equilibration time.

For both data sets, in water solutions and in water−ethanol solutions, the error bars are significantly larger at low concentrations. This is because the Einstein diffusion equation, eq 1, uses an average; therefore, one has inherently noisier results at low concentrations. Nevertheless, all simulations are well-converged with respect to time and have moderate time-averaged standard deviations. As a typical example, by taking only the first half of the data for the 1.1 M GdmCl in ∼1.1 M ethanol, we computed a diffusion coefficient $D = 5.9 \times 10^{-6}$ cm^2/s^{-1}, compared with $D = 6.2 \times 10^{-6}$ cm^2/s^{-1} for the full data set (Table 6), well within the standard deviation of 1.4×10^{-6} cm^2/s^{-1}.

TABLE 5: Measured[34] and Calculated Self-Diffusion Coefficient for Ethanol

	Ethanol Diffusion Coefficient (10^6 cm^2/s)
measured[34]	11.6 ± 0.3
calculated	11.0 ± 1.3

[a] Calculated values given are averaged over the last 1.6 ns of 2.1 ns trajectories, sampling every 10 ps for a total of 160 datapoints with time-averaged standard deviations also reported. Measured value includes $\pm 0.3 \times 10^{-6}$ cm^2/s estimated experimental error.[34]

TABLE 6: GdmCl Diffusion Coefficient (10^6 cm^2/s) in Water−Ethanol Solutions as a Function of Starting Ethanol Concentration (M)[a]

	[Ethanol], %			
	10	20	30	40
1.1 M GdmCl	6.2 ± 1.4	4.5 ± 1	3.6 ± 1	3.1 ± 0.7
2.2 M GdmCl	4.4 ± 0.8	3.9 ± 0.6	2.7 ± 0.6	2.4 ± 0.7

[a] The 16-molecule and 32-molecule GdmCl solutions are used, corresponding to approximately 1.1 and 2.2 M solute concentrations, respectively. Values given are averaged over the last 1.6 ns of 2.1 ns trajectories, sampling every 10 ps for a total of 160 datapoints with time-averaged standard deviations also reported. Similarly to the neat water solutions described above, equilibrated ethanol−water solution cell sizes decreased during equilibration to give slightly stronger equilibrated ethanol concentrations, with time-averaged equilibrated concentrations plotted in Figure 7.

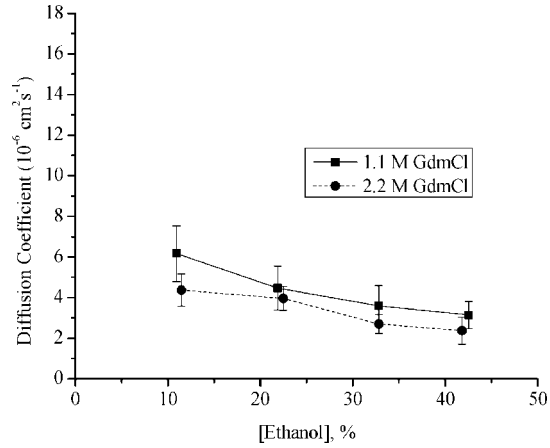

Figure 7. GdmCl diffusion in water−ethanol solutions as a function of ethanol concentration. The error bars represent time-averaged standard deviations, and datapoints for each data set are connected to guide the eye.

4. Conclusion

The concentration dependence of GdmCl diffusion in water and in water−ethanol solutions was computed, and results were validated against available experimental and simulation data. The diffusion properties determined from the simulations provide an important step toward optimizing the use of denaturants in protein unfolding studies and can, for example, be used as input for numerical modeling of denaturant concentration profiles in microfluidic cells. The insight gleaned into GdmCl diffusion and atom-scale dynamics also complements recent simulation work on the Gdm^+ interaction with peptides[36] and the structure of aqueous GdmCl solutions[33] and, more generally, the solvent-mediated interaction between hydrophobic surfaces in aqueous salt solutions,[37] as well as the influence of solvent chemical potential on protein structure.[38]

Acknowledgment. This work was funded by the EC NaPa project (Contract no. NMP4-CT-2003-500120). Calculations were performed at Tyndall National Institute by using computer resources provided by Science Foundation Ireland (SFI) and also at the SFI/HEA Irish Centre for High-End Computing (ICHEC). The authors thank David Mendels and Niall English for helpful discussions.

Supporting Information Available: Equilibration and detailed structural information for the GdmCl solution models. This material is available free of charge via the Internet at http://pubs.acs.org.

References and Notes

(1) Lim, C. T.; Zhang, Y. *Biosens. Bioelectron.* **2007**, *22*, 1197–1204.
(2) Dittrich, P. S.; Manz, A. *Nat. Rev. Drug Discovery* **2006**, *5*, 210–218.
(3) Pamme, N. *Lab. Chip* **2007**, *7*, 1644–1659.
(4) Reisner, W. W.; Beech, J. P.; Larsen, N. B.; Flyvbjerg, H.; Kristensen, A.; Tegenfeldt, J. O. *Phys. Rev. Lett.* **2007**, *99*, 058302.
(5) Whitby, M.; Quirke, N. *Nature Nanotech.* **2007**, *2*, 87–94.
(6) Wang, L.; Zhao, Y.; Ng, E.; Qiao, L. *Proc. IEEE Int. Conf. Microelectron. Mechanical Systems (MEMS 2005)* **2005**, 814–817.
(7) Helmke, B. P.; Minerick, A. R. *Proc. Natl. Acad. Sci. U.S.A.* **2006**, *103*, 6419–6424.
(8) Prusiner, S. B. *N. Engl. J. Med.* **2001**, *344*, 1516–1526.
(9) Foguel, D.; Silva, J. L. *Biochemistry* **2004**, *43*, 11361–11370.
(10) Stefani, M. *Biochim. Biophys. Acta* **2004**, *1739*, 5–25.
(11) Winklhofer, K. F.; Tatzelt, J.; Haass, C. *EMBO J.* **2008**, *27*, 336–349.
(12) Gosting, L. J.; Akeley, D. F. *J. Am. Chem. Soc.* **1952**, *74*, 2058–2060.
(13) Heil, S. R.; HoIz, M.; Kastner, T. M.; Weingartner, H. *J. Chem. Soc., Faraday Trans.* **1995**, *91*, 1877–1880.
(14) Weerasinghe, S.; Smith, P. E. *J. Chem. Phys.* **2004**, *121*, 2180–2186.
(15) Guillot, B. J. *J. Mol. Liq.* **2002**, *101*, 219–260.
(16) Turoverov, K. K.; Verkhusha, V. V.; Shavlovsky, M. M.; Biktashev, A. G.; Povarova, O. I.; Kuznetsova, I. M. *Biochemistry* **2002**, *41*, 1014–1019.
(17) Sasahara, K.; Katsutoshi, N. *Proteins: Struct., Funct., Bioinf.* **2006**, *63*, 127–135.
(18) O'Mahony, K.; Freitag, R.; Hilbrig, F.; Schumacher, I.; Müller, P. *Biotechnol. Prog.* **2007**, *23*, 895–903.
(19) Christel, L. A.; Petersen, W.; McMillan, W.; Northup, M. A. *J. Biomech. Eng.-T ASME* **1999**, *121*, 22–27.
(20) Juyal, P.; Anand, O. N. *Fuel* **2003**, *82*, 97–103.
(21) Greene, R. F.; Pace, C. N. *J. Biol. Chem.* **1974**, *249*, 5388–5393.
(22) Ladurner, A. G.; Itzhaki, L. S.; Daggett, V.; Fersht, A. R. *Proc. Natl. Acad. Sci. U.S.A.* **1998**, *95*, 8473–8478.
(23) Yoda, T.; Saito, M.; Arai, M.; Horii, K.; Tsumoto, K.; Matsushima, M.; Kumagai, I.; Kuwajima, K. *Proteins: Struct., Funct., Bioinf.* **2001**, *42*, 49–65.
(24) MacKerrell, A. D.; Bashford, D.; Bellott, M.; Dunbrack, D. L.; Evanseck, J. D.; Field, M. J. *J. Phys. Chem. B* **1998**, *102*, 3586–3616.
(25) Ryckaert, J. P.; Ciccotti, G.; Berendsen, H. J. C. *J. Comput. Phys.* **1977**, *23*, 327–341.
(26) Brooks, B. R.; Bruccoleri, R. E.; Olafson, B. D.; States, D. J.; Swaninathan, S.; Karplus, M. *J. Comput. Chem.* **1983**, *4*, 187–217.
(27) English, N. J. *Mol. Phys.* **2005**, *103*, 1945–1960.
(28) Jorgensen, W. L.; Chandrasekhar, J.; Madura, J. D.; Impey, R. W.; Klein, M. L. *J. Chem. Phys.* **1983**, *79*, 926–935.
(29) Horn, H. W.; Swope, W. C.; Pitera, J. W.; Madura, J. D.; Dick, T. J.; Hura, G. L.; Head.Gordon, T. *J. Chem. Phys.* **2004**, *120*, 9665–9678.
(30) Mills, R. *J. Phys. Chem.* **1973**, *77*, 685–688.
(31) Kawahara, K.; Tanford, C. *J. Biol. Chem.* **1966**, *241*, 3228–3232.
(32) Dill, K. A.; Bromberg, S. *Molecular Driving Forces*; Garland Science: New York, 2003; pp 327−328.
(33) Mason, P. E.; Neilson, G. W.; Enderby, J. E.; Saboungi, M. L.; Dempsey, C. E.; MacKerell, A. D.; Brady, J. W. *J. Am. Chem. Soc.* **2004**, *126*, 11462–11470.
(34) Pratt, K. C.; Wakeham, W. A. *J. Chem. Soc., Faraday Trans. 2* **1977**, *73*, 997–1002.
(35) Johnson, T. J.; Ross, D.; Locascio, L. E. *Anal. Chem.* **2002**, *74*, 45–51.
(36) Mason, P. E.; Brady, J. W.; Neilson, G. W.; Dempsey, C. E. *Biophys. J.* **2007**, *93*, L04–L06.
(37) Zangi, R.; Hagen, M.; Berne, B. J. *J. Am. Chem. Soc.* **2007**, *129*, 4678–4686.
(38) Timasheff, S. N. *Proc. Natl. Acad. Sci. U.S.A.* **2002**, *99*, 9721–9726.

JP8030336